BMB
reports

Analysis of the solution structure of the human antibiotic peptide dermcidin and its interaction with phospholipid vesicles

Hyun Ho Jung[1], Sung-Tae Yang[2], Ji-Yeong Sim[1], Seungkyu Lee[1], Ju Yeon Lee[1], Ha Hyung Kim[3], Song Yub Shin[4] & Jae Il Kim[1,]*

[1]Department of Life Science, Gwangju Institute of Science and Technology, Gwangju, [2]Section on Membrane Biology, Laboratory of Cellular and Molecular Biophysics, National Institute of Child Health and Human Development, National Institutes of Health, Bethesda, MD 20892, [3]College of Pharmacy, Chung-Ang University, Seoul, [4]Department of Bio-Materials, Graduate School and Department of Cellular & Molecular Medicine, School of Medicine, Chosun University, Gwangju 501-759, Korea

Dermcidin is a human antibiotic peptide that is secreted by the sweat glands and has no homology to other known antimicrobial peptides. As an initial step toward understanding dermcidin's mode of action at bacterial membranes, we used homonuclear and heteronuclear NMR to determine the conformation of the peptide in 50% trifluoroethanol solution. We found that dermcidin adopts a flexible amphipathic α-helical structure with a helix-hinge-helix motif, which is a common molecular fold among antimicrobial peptides. Spin-down assays of dermcidin and several related peptides revealed that the affinity with which dermcidin binds to bacterial-mimetic membranes is primarily dependent on its amphipathic α-helical structure and its length (>30 residues); its negative net charge and acidic pI have little effect on binding. These findings suggest that the mode of action of dermcidin is similar to that of other membrane-targeting antimicrobial peptides, though the details of its antimicrobial action remain to be determined [BMB reports 2010; 43(5): 362-368]

INTRODUCTION

Antimicrobial peptides are produced in a wide range of animals for innate host defense and show a broad spectrum of antimicrobial activity (1-4). Despite the remarkable diversity of their amino acid compositions, antimicrobial peptides show several common features, including the presence of multiple basic amino acids and amphipathic structures with clusters of hydrophobic and hydrophilic amino acids (5-8). Recent studies of the modes of action of various antimicrobial peptides have revealed that their cationic nature contributes to their initial binding to negatively charged bacterial membranes through electrostatic interaction, while their amphipathic structures enhance peptide-lipid interactions at the water-bilayer interface, ultimately leading to cell death via pore formation or membrane disintergration (9-14).

Dermcidin (DCD) is an antimicrobial peptide found in human sweat. It is produced through proteolytic processing of a 110-amino acid precursor protein that has no homology to other known antimicrobial peptides (15, 16). The processed peptide, DCD-1, has 47 amino acids and shows a broad spectrum of antimicrobial activity against a variety of pathogenic microorganisms (15, 17, 18). Using immune-EM, it was recently shown that the antimicrobial activity of DCD-1 originates with its binding to the bacterial membrane, and that it effectively kills *Staphylococcus epidermidis* (18).

DCD-1L, which is produced by adding a leucine residue to the C-terminus of DCD-1, shows stronger antimicrobial activity than the parent peptide (15). It is especially noteworthy that DCD-1L exhibits activity against drug-resistant *S. aureus*, as well as other Gram-positive and Gram-negative bacterial strains (17). In the present study, we used nuclear magnetic resonance (NMR) spectroscopy to determine, for the first time, the solution structure of DCD-1L in a bacterial membrane- mimetic environment. In addition, to investigate the interaction between DCD-1L and bacterial membranes, we synthesized a set of six DCD-derived peptides, including DCD-1 and five fragments, and then performed spin-down assays to assess their binding to bacterial-mimetic membranes. Our findings suggest that the affinity with which DCD binds to bacterial membranes reflects its amphipathic helical content and its length (>30 residues); its negative net charge and acidic pI had little effect on binding.

*Corresponding author. Tel: 82-62-970-2494; Fax: 82-62-970-2484; E-mail: jikim@gist.ac.kr

Received 8 April 2010, Accepted 15 April 2010

Keywords: Amphipthic α-helical structure, Antimicrobial peptide, Helix-hinge-helix motif, Nuclear magnetic resonance (NMR) spectroscopy, Peptide-membrane interaction

RESULTS AND DISCUSSION

Expression and purification of DCD

To investigate the solution structure of DCD using NMR spectroscopy, DCD-1L was produced and labeled with a stable isotope using an *E. coli* expression system. Synthetic DNA encoding DCD-1L was cloned into pET31.b(+) expression vector, also encoding a ketosteroid isomerase (KSI) fusion partner, and a methionine residue for CNBr cleavage was inserted between the KSI and DCD-1L. Although DCD-1L shows cytotoxic activity against *E. coli*, SDS-PAGE showed that formation of a recombinant KSI fusion protein enabled its expression in an inclusion body. Thereafter the inclusion bodies were collected, and the fusion protein was cleaved using CNBr with 70% formic acid. Release of DCD-1L from the fusion protein was confirmed by SDS-PAGE, and the peptide was then purified using RP-HPLC. To label DCD-1L with a stable isotope, these optimized processes were performed in M9 minimal medium containing $^{15}NH_4Cl$. Both DCD-1L and uniformly ^{15}N-labeled DCD-1L showed the expected molecular masses in matrix-assisted laser desorption/ionization time-of-flight mass spectrometry (MALDI-TOF MS) analyses (4818.5 Da and 4875.5 Da, respectively).

Structural analysis of DCD using CD spectroscopy

The secondary structure of DCD-1L was analyzed using circular dichroism (CD) spectroscopy. CD spectra were collected in 50 mM sodium phosphate buffer, 20 mM SDS and 50% trifluoroethanol (TFE) (Fig. 1A). In the sodium phosphate buffer, the DCD-1L spectrum had a broad negative band at about 200 nm, which is frequently observed in random coil or β-sheet structures with no α-helix. In the presence of either SDS micelles or TFE solution, however, the CD spectra for DCD1L exhibited a typical α-helical CD pattern, with minimal mean residue molar ellipticity values of 208 and 222 nm. Although there was an appreciable difference between the CD helical contents of DCD-1L in 20 mM SDS micelles and 50% TFE, it is noteworthy that the peptide has no homology to other known antimicrobial peptides, yet in membrane-mimetic environments it showed a typical α-helical structure, which is characteristic of a variety of antimicrobial peptides (19-22).

NMR analysis and structural calculation of DCD

To overcome ambiguity in the CD analysis, we next carried out an NMR structural analysis of DCD-1L. We chose to use 50% TFE as the solvent over 100 mM SDS micelles because all of the signals were well dispersed, without severe overlapping of the NMR peaks. Complete sequence-specific resonance as-

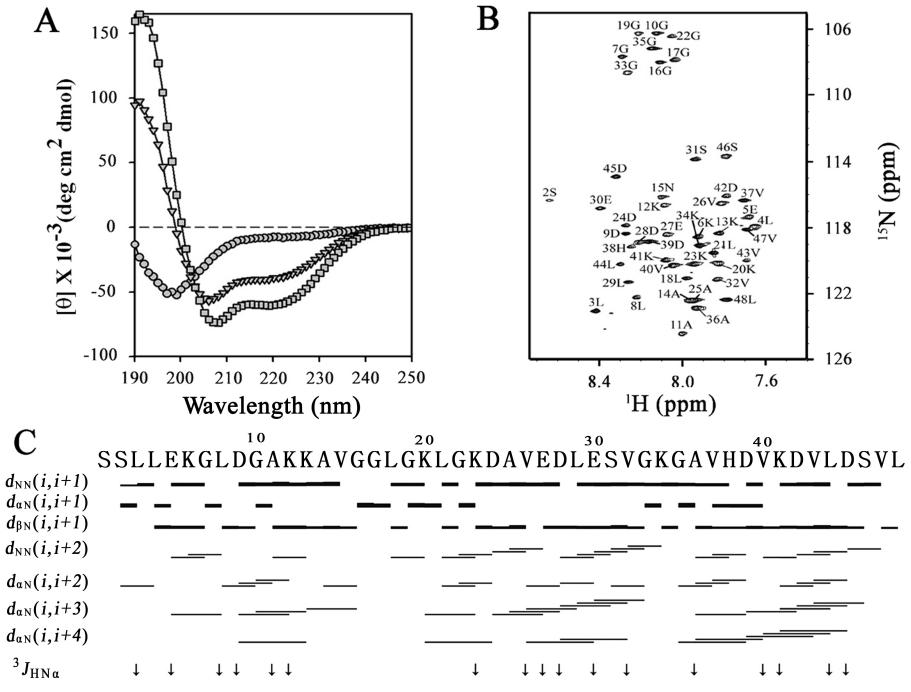

Fig. 1. (A) CD spectra for 50 μM DCD-1L in 50 mM sodium phosphate buffer (○), 20 mM SDS micelles (□) and 50% TFE (△). (B) ^{1}H-^{15}N HSQC spectrum for DCD-1L in 50% TFE. Backbone amide protons are labeled with the residue number using standard single-letter amino acid abbreviations. (C) Summary of the sequential NOE connectivities and $^{3}J_{HN\alpha}$ coupling constants. The thickness of the NOE lines corresponds to the intensity of the NOE connectivities. The values of the $^{3}J_{HN\alpha}$ coupling constants are indicated by ↑ (>8 Hz) and ↓ (<5.5 Hz).

signments (Fig. 1B) were established from 3D ^{15}N-TOCSY-HSQC and ^{15}N-NOESY-HSQC, combined with a series of 2D analyses (DQF-COSY, TOCSY and NOESY). Identification of the amino acid spin system was based on scalar coupling patterns observed in 3D ^{15}N-TOCSY-HSQC, 2D DQF-COSY and 2D TOCSY. The identified spin systems were arranged along the primary structure of the peptide using interresidue sequential NOEs observed in the ^{15}N-NOESY-HSQC spectrum, and the pattern of observed NOEs was ultimately interpreted in terms of the secondary structure of the molecule. As summarized in Fig. 1C, the small $^{3}J_{HN\alpha}$ coupling constants, $d_{NN}(i,i+2)$, $d_{\alpha N}(i,i+3)$, $d_{\alpha N}(i,i+4)$, and strong $d_{NN}(i,i+1)$ NOE connectivity indicate that DCD-1L contains four α-helices as secondary structural elements: Glu5-Gly7, Gly10-Lys12, Glu27-Ser31 and Val37-Val43.

To calculate the 3D structure of DCD-1L, we used a total of 273 constraints that included 256 interresidue distance constraints from NOE cross peaks and 17 dihedral angle constraints from the coupling constants, which correspond to a poor average of 5.8 constraints per residue. After carrying out the simulated annealing calculations starting with 100 random structures, the 20 final structures were selected based on the lowest CYANA target function and were further refined using CNS with a water shell refinement protocol. The average CYANA target function for the 20 final structures was 0.12 ± 0.0779 Å. With the exception of two helical segments (Asp24 to Ser31 and Ala36 to Ser46), the molecule was little affected by the NMR constraints, reflecting the randomness of the conformationally disordered backbone (Fig. 2A, B). The structural statistics for the 20 lowest energy structures indicated that the atomic root mean square deviations for the mean coordinate positions for residues Asp24 to Ser31 and Ala36 to Ser46 were 0.79 ± 0.24 Å and 0.79 ± 0.21 Å, respectively, for the backbone atoms (N, C^{α}, and C) and 1.73 ± 0.26 Å and 1.82 ± 0.32 Å, respectively, for all heavy atoms. In a Ramachandran analysis using the program PROCHECK-NMR, the backbone dihedral angles for all of the residues in the 20 final structures fell either in most favored regions or in additionally allowed regions. On the basis of these findings, we suggest that the DCD molecule is highly flexible, even in membrane-mimetic TFE solution, and this inherent flexibility of the DCD-1L molecule is likely reflected by the absence of medium- and long-range NOE constraints.

Molecular profile of DCD

The molecular structure of DCD-1L shows an overall topology that consists of four α-helices and several turns (Fig. 2C). The four α-helices are formed by residues Glu5 to Gly7 (α-helix I), Gly10 to Lys12 (α-helix II), Glu27 to Ser31 (α-helix III) and Val37 to Val43 (α-helix IV), and several type IV β-turns (miscellaneous type) were observed in the regions that involve residues Glu5 to Leu8, Gly17 to Lys20, Lys20 to Lys23, Leu21 to Asp24 and Gly33 to Ala36. Among the 20 final structures, α-helixes I-IV occurred in only 8, 14, 13 and 11 structures, respectively, which is consistent with the DCD molecule's high degree of flexibility. Within the solution structure, the N-terminal half of DCD-1L (Ser1 to Lys23) was less restricted by the NMR constraints than the C-terminal half (Asp24 to Leu48). The primary sequence of the N-terminal half of DCD-1L contains six glycines (Gly7, Gly10, Gly16, Gly17, Gly19 and Gly22), which likely explains the flexibility of the N-terminal portion of DCD-1L. By contrast, the C-terminal half of DCD1L has only two glycines (Gly33 and Gly35), which form a type IV β-turn connecting α-helix III (Asp24 to Ser31) and α-helix IV (Ala36 to Ser46).

The amphipathic nature of the helix in DCD-1L is repre-

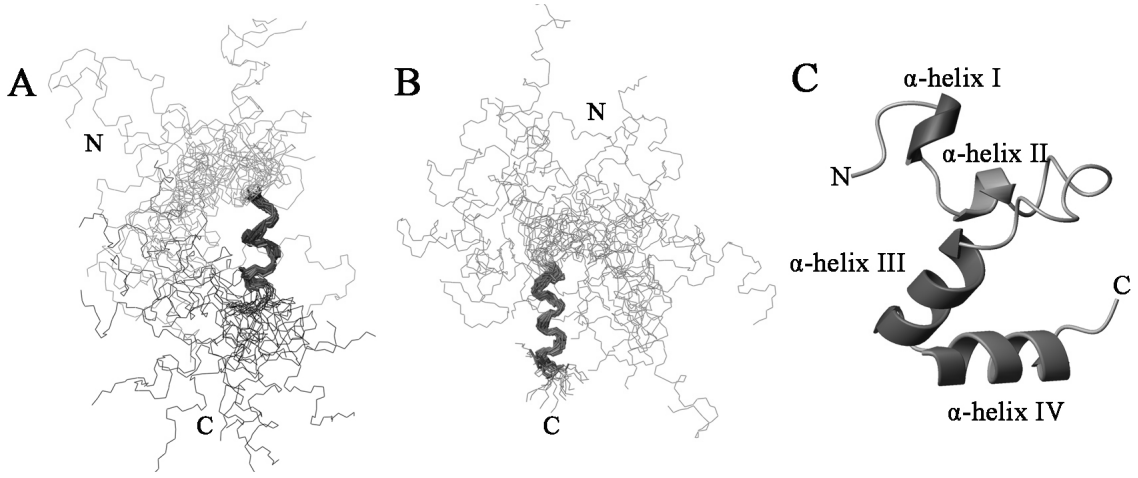

Fig. 2. Structure of DCD-1L in 50% TFE. The backbone heavy atoms of 20 converged DCD-1L structures are superimposed at residues 24-31 (A) and 36-46 (B). (C) Ribbon model of the structure of DCD-1L. α-helixes I, II, III and IV are shown in red, orange, purple and green, respectively. All figures were generated using MOLMOL.

sented as three separated regions in Fig. 3. The first region (Ser1-Leu18) includes helixes I and II (Fig. 3A), which are relatively short helixes, while the second (Gly19-Val32) and third (Gly33-Leu48) regions include helix III (Fig. 3B) and helix IV (Fig. 3C), respectively, which are relatively long. As shown in Fig. 3, it is clear that the charged residues are clustered on one side of helix, while the hydrophobic residues are clustered on the other side; thus the structure of DCD-1L is amphipathic in an environment mimicking the bacterial membrane (23-25).

Membrane interaction of DCD and its fragments

DCD-1 is comprised of 47 amino acids and shows antimicrobial activity against a variety of pathogenic microorganisms (15, 17, 18). It was recently reported that although the antimicrobial activity of DCD-1 originates with its binding to bacterial membranes, the bacterial membrane not very permeable to DCD-1 (18). To investigate the interaction between DCD-1 and the bacterial membrane in more detail, we carried out structure-based analysis using the NMR solution structure as a model and synthesized seven DCD-derived peptides, including DCD-1, DCD-1L and five DCD fragments (Table 1). Among the fragments, DCD (1-16) included helixes I and II (Fig. 3A); DCD (17-32) and DCD (33-47) included helixes III (Fig. 3B) and IV (Fig. 3C), respectively; DCD (1-32) consisted of the sequences of DCD (1-16) plus DCD (17-32); and DCD (17-47) consisted of the sequences of DCD (17-32) plus DCD (33-47). In spin-down assays, we then analyzed the membrane partitioning of each peptide in bacterial-mimetic model membranes (POPC : POPG, 1 : 1 molar ratio). As shown in Fig. 3D and E, the model membrane was very effective for assessing peptide binding to lipid vesicles in the aqueous phase. The partition coefficients (K_x) for DCD-1L and DCD-1 were 5.11×10^5 and 1.67×10^5, respectively (Table 1). Although the DCD-1L sequence only adds a C-terminal leucine residue to the DCD-1 sequence, DCD-1L binds to the bacterial-mimetic membranes with about three-fold greater affinity than DCD-1. By contrast, with K_x values of 9.38×10^2, 6.67×10^3 and 2.65×10^3, respectively, DCD (1-16), DCD (17-32) and DCD (33-47) showed significantly less affinity for bacterial-mimetic membranes than wild-type DCD (Table 1). Notably, DCD (1-32) and DCD (17-47) exhibited similar K_x values (1.05×10^5 and 2.17×10^5, respectively) that were also similar to the Kx of full-length DCD-1.

It is well known that the functional activity of antimicrobial peptides against bacterial strains is determined by complex interactions involving their cationicity, hydrophobicity, α–helixity and amphipathicity. Although DCD has a net charge of −2 and an acidic pI value, we found that neither of these characteristics significantly affected its binding to bacterial-mimetic membranes. Our findings thus suggest that the binding of DCD to bacterial membranes is dependent on the peptide's amphipathic structure, its length (>30 residues) and its helical

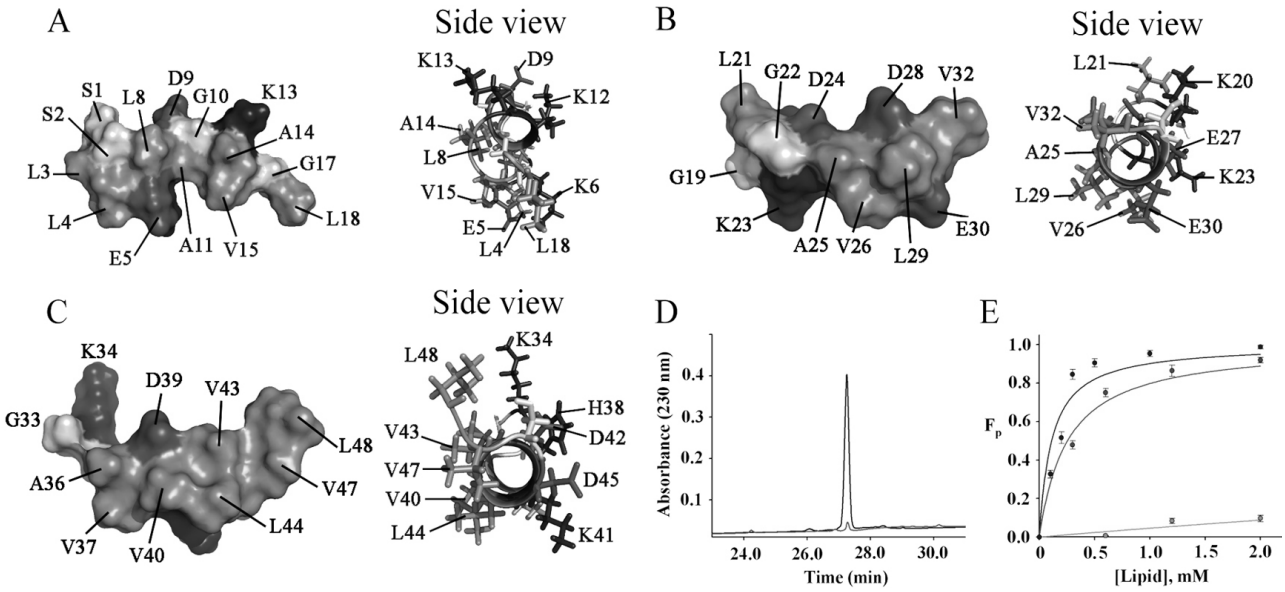

Fig. 3. Regional surface models of DCD-1L in 50% TFE and its interaction with lipid vesicles. (A-C) Surface profiles the regions spanning Ser1-Leu18 (A), Gly19-Val32 (B) and Gly33-Leu48 (C) are shown. The hydrophobic, basic and acidic residues are shown in green, blue and red, respectively. (D) RP-HPLC traces showing the levels of DCD-1L in supernatant after ultracentrifugation of DCD-1L suspensions in the absence (black) and presence of 0.3 mM POPC : POPG (1 : 1) lipid vesicles (red). (E) Fraction of DCD-1L (blue), DCD (17-47) (red) and DCD (33-47) (green) partitioned into vesicles (Fp) plotted as a function of the concentration of available lipid. Smooth curves were obtained by fitting with the equation presented in the Materials and Methods.

Table 1. Amino acid sequences, net charge/pI values, and partition coefficients (Kx) of DCD-1L and its fragments

Name	Sequence	Charge/pI	K_x
DCD-1L	SSLLEKGLDGAKKAVGGLGKLGKDAVEDLESVGKGAVHDVKDVLDSVL	−2/5.07	5.11×10^5
DCD-1	SSLLEKGLDGAKKAVGGLGKLGKDAVEDLESVGKGAVHDVKDVLDSV	−2/5.07	1.67×10^5
DCD (1-16)	SSLLEKGLDGAKKAVG	+1/8.22	9.38×10^2
DCD (17-32)	GLGKLGKDAVEDLESV	−2/4.32	6.67×10^3
DCD (33-47)	GKGAVHDVKDVLDSV	−1/5.30	2.65×10^3
DCD (1-32)	SSLLEKGLDGAKKAVGGLGKLGKDAVEDLESV	−1/4.99	1.05×10^5
DCD (17-47)	GGLGKLGKDAVEDLESVGKGAVHDVKDVLDSV	−3/4.59	2.17×10^5

content; not its net charge or pI. This is consistent with an earlier report suggesting the antimicrobial activity of DCD peptides is independent of their net charge (18).

The structure of DCD includes a highly flexible N-terminal helical region and a relatively ordered C-terminal helical region. A structural homology search based on the helix-hinge-helix motif suggests DCD resembles a variety of antimicrobial peptides, including cecropin A, gaegurin 4 (GGN4) and SMAP-29 (23, 26, 27). DCD-1L shows particular similarity to SMAP-29, an antimicrobial peptide from sheep (27) that presents a flexible N-terminal region (residues 1 to 6), a helical region (residues 8 to 17), a C-terminal helical region (residues 20 to 28) and a hinge segment (Gly18 and Pro19). Interestingly, both the N- and C-terminal regions of SMAP-29 participate in binding to lipopolysaccharide (LPS) on the bacterial surface membrane. Although DCD's antibacterial mechanism of action remains unknown, it is unlikely that the flexible N-terminal region of DCD-1L is directly involved in LPS-binding, as DCD (1-32) and DCD (17-47) partitioned similarly. Still, our structural analysis suggests DCD likely acts in a manner similar to that of other membrane-targeting antimicrobial peptides that adopt amphipathic α-helical structures with helix-hinge-helix motifs, which is a common molecular fold among antimicrobial peptides, irrespective of their amino acid sequences and net charges.

MATERIALS AND METHODS

Cloning and purification of uniformly ^{15}N-labeled DCD-1L

A synthetic DNA fragment encoding DCD-1L was cloned into pET31.b(+) expression vector (Novagen), and the recombinant protein, along with a ketosteroid isomerase (KSI) fusion partner, was expressed in *E. coli* BL21 (DE3) strain (Novagen) (28). The cells were cultured in 50 ml of Luria-Bertani (LB) medium containing ampicillin (100 mg/ml) until transferred to 1 L of M9 minimal medium containing $^{15}NH_4Cl$. After induction with IPTG (100 mg/L) for 5 h at 37°C, the cells were harvested, lysed and spun down. The resultant pellets, which included the recombinant fusion protein, were collected and treated with CNBr cleavage buffer, after which the cleaved sample was diluted 10-fold in deionized water. DCD-1L was then purified from the sample using reverse phase-high performance liquid chromatography (RP-HPLC) with an ODS (C-18) column (4.6 × 250 mm, Shimadzu), and its molecular weight was confirmed using MALDI-TOF MS (Shimadzu).

Synthesis of DCD-1 and its fragments

DCD-1 and its fragments were synthesized using the solid phase method with Fmoc (fluoren-9-yl-methoxycarbonyl)-chemistry. Fmoc-protected peptides were deprotected and cleaved using a mixture of TFA (trifluoroacetic acid), phenol, water, thioanisole and 1,2-ethandithiol (82.5 : 5 : 5 : 5 : 2.5, v/v) for 4 h at room temperature. The synthetic peptides were then purified by RP-HPLC using an ODS column (4.6 × 250 mm, Shimadzu), after which the purity (~98%) of the peptides was confirmed by analytical HPLC, and the molecular weights of the synthetic peptides were confirmed by MALDI-TOF MS (Shimadzu).

CD spectra

CD spectra were recorded using a J-715 CD spectrophotometer (Jasco) with a 1-mm path length cell. Wavelengths were measured from 190 to 250 nm at 50 nm/min, with a step resolution of 0.1 nm, a response time of 0.5 s and a bandwidth of 1 nm. The CD spectra were collected and averaged over 4 scans in 50 mM sodium phosphate buffer (pH 5.8), 20 mM SDS or 50% TFE. The mean residue ellipticity [θ] (given in deg · cm^2 · $dmol^{-1}$) was calculated as [θ] = [θ]obs (MRW/10lc), where [θ]obs is the ellipticity measured in millidegres, MRW is the mean residue molecular weight of the target protein, c is the concentration of the sample in mg/ml, and l is the optical path length of the cell in cm. The spectra were plotted as molar ellipticity [θ] against wavelength.

NMR experiments

For the NMR experiments, samples were dissolved with 100 mM SDS buffer or 50% TFE, and all experiments were conducted on a Bruker AVANCE 600 spectrometer at 298 K and pH 4.2. For 2D NMR, samples were prepared at a concentration of 1 mM, and their 2D standard spectra (DQF-COSY, TOCSY, NOESY) were measured. TOCSY and NOESY spectra were recorded with mixing times of 80 and 100-200 ms. For 3D NMR, ^{15}N-labeled samples were dissolved to 0.5 mM in each buffer, and 2D ^{1}H-^{15}N HSQC, 3D ^{15}N-TOCSY-HSQC and

3D ^{15}N-NOESY-HSQC spectra were recorded. The mixing times for 3D ^{15}N-TOCSY-HSQC and ^{15}N-NOESY-HSQC spectra were 80 ms and 150 ms. The $^{3}J_{HN\text{-}H\alpha}$ values were obtained from the 3D HNHA spectrum. TSP was used as a reference for ^{1}H chemical shifts, and ^{15}N chemical shifts were calculated from the ^{1}H frequency. All spectra were processed using XWIN-NMR 3.5 and analyzed using SPARKY.

Structure calculation

The distance and dihedral angle constraints used for structure calculation were obtained from the 3D ^{15}N-NOESY-HSQC and 3D HNHA spectra. The backbone NH-C$^{\alpha}$H coupling constants were converted to backbone torsion angle θ constraints using the following rules. For $^{3}J_{NH\text{-}C\alpha H}$ values <5.5 Hz, the θ angle was constrained in the range of $-60^{o} \pm 30^{o}$; for $^{3}J_{NH\text{-}C\alpha H}$ values >8.0 Hz, it was constrained in the range of $-120^{o} \pm 40^{o}$. On the basis of these constraints, structure calculations were carried out using CYANA 2.1 with torsion angle dynamics (29). Twenty structures were calculated from 100 randomized structures based on the target function and processed with water refinement and molecular dynamics simulations using CNS (30). The qualities of the 20 final structures were analyzed using PROCHECK_NMR and PROMOTIF, and visualized using MOLMOL and PyMOL. Finally, the atomic coordinates for the converged structures of DCD-1L were deposited in the Protein Data Bank (PDB ID: 2ksg)

Spin-down assays

The interactions of DCD and its fragments with small unilamellar vesicles (SUVs) were evaluated using spin-down assays. Phospholipids [POPC/POPG (1 : 1)] were dissolved in chloroform and then converted to a thin lipid film by drying overnight in a stream of nitrogen gas under vacuum. The phospholipid was then resuspended an aqueous buffer containing 10 mM Tris (pH 7.4), 0.1 mM EDTA and 150 mM NaCl by vortex mixing. To calculate the partition coefficients (K_x) of the peptides in spin-down assays, various amounts of SUVs were incubated in an aqueous solution of DCD-1L or one of its fragments (2 mg/ml) for 1 h at room temperature, after which the lipid vesicles were separated by centrifugation (1 h, 100,000 g). The amount of peptide remaining in the aqueous phase was determined by RP-HPLC. K_x values were calculated as $F_p = (K_x[\text{lipid}])/(K_x[\text{lipid}] + [\text{water}])$, where $F_p = ([\text{Peptide}_{total}] - [\text{Peptide}_{free}])/[\text{Peptide}_{total}]$.

Acknowledgements

This study was supported by grants from the Brain Research Center of the 21st Century Frontier Research Program (M103 KV010006-06K2201-00610), the BioImaging Research Center at GIST, and the Korea Healthcare Technology R&D Project, Ministry of Health & Welfare, Republic of Korea (A080712).

REFERENCES

1. Zasloff, M. (2002) Antimicrobial peptides of multicellular organisms. *Nature* **415**, 389-395.
2. Selsted, M. E. and Ouellette, A. J. (2005) Mammalian defensins in the antimicrobial immune response. *Nat. Immunol.* **6**, 551-557.
3. Ganz, T. and Lehrer, R. I. (1998) Antimicrobial peptides of vertebrates. *Curr. Opin. Immunol.* **10**, 41-44.
4. Finlay, B. B. and Hancock, R. E. (2004) Can innate immunity be enhanced to treat microbial infections? *Nat. Rev. Microbiol.* **2**, 497-504.
5. Epand, R. M. and Vogel, H. J. (1999) Diversity of antimicrobial peptides and their mechanisms of action. *Biochim. Biophys. Acta.* **1462**, 11-28.
6. Bulet, P., Stocklin, R. and Menin, L. (2004) Anti-microbial peptides: from invertebrates to vertebrates. *Immunol. Rev.* **198**, 169-184.
7. Tossi, A., Sandri, L. and Giangaspero, A. (2000) Amphipathic, alpha-helical antimicrobial peptides. *Biopolymers.* **55**, 4-30.
8. Hancock, R. E. and Scott, M. G. (2000) The role of antimicrobial peptides in animal defenses. *Proc. Natl. Acad. Sci. U.S.A.* **97**, 8856-8861.
9. Huang, H. W. (2000) Action of antimicrobial peptides: two-state model. *Biochemistry.* **39**, 8347-8352.
10. Yang, L., Harroun, T. A., Weiss, T. M., Ding, L. and Huang, H. W. (2001) Barrel-stave model or toroidal model? A case study on melittin pores. *Biophys. J.* **81**, 1475-1485.
11. Matsuzaki, K., Sugishita, K., Ishibe, N., Ueha, M., Nakata, S., Miyajima, K. and Epand, R. M. (1998) Relationship of membrane curvature to the formation of pores by magainin 2. *Biochemistry.* **37**, 11856-11863.
12. Christensen, B., Fink, J., Merrifield, R. B. and Mauzerall, D. (1988) Channel-forming properties of cecropins and related model compounds incorporated into planar lipid membranes. *Proc. Natl. Acad. Sci. U.S.A.* **85**, 5072-5076.
13. Shai, Y. and Oren, Z. (2001) From "carpet" mechanism to de-novo designed diastereomeric cell-selective antimicrobial peptides. *Peptides.* **22**, 1629-1641.
14. Ladokhin, A. S. and White, S. H. (2001) 'Detergent-like' permeabilization of anionic lipid vesicles by melittin. *Biochim. Biophys. Acta.* **1514**, 253-260.
15. Schittek, B., Hipfel, R., Sauer, B., Bauer, J., Kalbacher, H., Stevanovic, S., Schirle, M., Schroeder, K., Blin, N., Meier, F., Rassner, G. and Garbe, C. (2001) Dermcidin: a novel human antibiotic peptide secreted by sweat glands. *Nat. Immunol.* **2**, 1133-1137.
16. Flad, T., Bogumil, R., Tolson, J., Schittek, B., Garbe, C., Deeg, M., Mueller, C. A. and Kalbacher, H. (2002) Detection of dermcidin-derived peptides in sweat by ProteinChip technology. *J. Immunol. Methods.* **270**, 53-62.
17. Lai, Y. P., Peng, Y. F., Zuo, Y., Li, J., Huang, J., Wang, L. F. and Wu, Z. R. (2005) Functional and structural characterization of recombinant dermcidin-1L, a human antimicrobial peptide. *Biochem. Biophys. Res. Commun.* **328**, 243-250.
18. Steffen, H., Rieg, S., Wiedemann, I., Kalbacher, H., Deeg, M., Sahl, H. G., Peschel, A., Gotz, F., Garbe, C. and

Schittek, B. (2006) Naturally processed dermcidin-derived peptides do not permeabilize bacterial membranes and kill microorganisms irrespective of their charge. *Antimicrob. Agents. Chemother.* **50**, 2608-2620.
19. Matsuzaki, K. (1998) Magainins as paradigm for the mode of action of pore forming polypeptides. *Biochim. Biophys. Acta.* **1376**, 391-400.
20. Simmaco, M., Mignogna, G. and Barra, D. (1998) Antimicrobial peptides from amphibian skin: what do they tell us? *Biopolymers.* **47**, 435-450.
21. Gazit, E., Lee, W. J., Brey, P. T. and Shai, Y. (1994) Mode of action of the antibacterial cecropin B2: a spectrofluorometric study. *Biochemistry.* **33**, 10681-10692.
22. Oren, Z. and Shai, Y. (1998) Mode of action of linear amphipathic alpha-helical antimicrobial peptides. *Biopolymers.* **47**, 451-463.
23. Holak, T. A., Engstrom, A., Kraulis, P. J., Lindeberg, G., Bennich, H., Jones, T. A., Gronenborn, A. M. and Clore, G. M. (1988) The solution conformation of the antibacterial peptide cecropin A: a nuclear magnetic resonance and dynamical simulated annealing study. *Biochemistry.* **27**, 7620-7629.
24. Katsu, T., Kuroko, M., Morikawa, T., Sanchika, K., Yamanaka, H., Shinoda, S. and Fujita, Y. (1990) Interaction of wasp venom mastoparan with biomembranes. *Biochim. Biophys. Acta.* **1027**, 185-190.
25. Oh, D., Shin, S. Y., Lee, S., Kang, J. H., Kim, S. D., Ryu, P. D., Hahm, K. S. and Kim, Y. (2000) Role of the hinge region and the tryptophan residue in the synthetic antimicrobial peptides, cecropin A(1-8)-magainin 2(1-12) and its analogues, on their antibiotic activities and structures. *Biochemistry.* **39**, 11855-11864.
26. Park, S. H., Kim, Y. K., Park, J. W., Lee, B. and Lee, B. J. (2000) Solution structure of the antimicrobial peptide gaegurin 4 by ^{1}H and ^{15}N nuclear magnetic resonance spectroscopy. *Eur. J. Biochem.* **267**, 2695-2704.
27. Tack, B. F., Sawai, M. V., Kearney, W. R., Robertson, A. D., Sherman, M. A., Wang, W., Hong, T., Boo, L. M., Wu, H., Waring, A. J. and Lehrer, R. I. (2002) SMAP-29 has two LPS-binding sites and a central hinge. *Eur. J. Biochem.* **269**, 1181-1189.
28. Cipakova, I., Gasperik, J. and Hostinova, E. (2006) Expression and purification of human antimicrobial peptide, dermcidin, in *Escherichia coli*. *Protein. Expr. Purif.* **45**, 269-274.
29. Guntert, P. (2004) Automated NMR structure calculation with CYANA. *Methods. Mol. Biol.* **278**, 353-378.
30. Brunger, A. T., Adams, P. D., Clore, G. M., DeLano, W. L., Gros, P., Grosse-Kunstleve, R. W., Jiang, J. S., Kuszewski, J., Nilges, M., Pannu, N. S., Read, R. J., Rice, L. M., Simonson, T. and Warren, G. L. (1998) Crystallography & NMR system: a new software suite for macromolecular structure determination. *Acta. Crystallogr. D. Biol. Crystallogr.* **54**, 905-921.